JOURNAL OF APPLIED ELECTROCHEMISTRY 9 (1979) 437–444

Dispersion in electrochemical cells with radial flow between parallel electrodes. II. Experimental results for capillary gap cell and pump cell configurations

M. FLEISCHMANN, J. GHOROGHCHIAN, R. E. W. JANSSON

Chemistry Department, Southampton University, UK

Received 15 May 1978; in revised form 6 March 1979

The dispersive plug flow mathematical model derived in the previous paper has been applied to experimental data obtained in model cells. Even though the results are approximate it is shown that the local mixing environment close to an electrode, and the segregation of the wall layer from the core flow, are dependent upon a number of operating variables, one of which is the direction of flow. The insight gained can be used to explain the distribution of products in a number of electrosynthetic reactions.

List of Symbols

$\bar{D}$	dispersion coefficient ($cm^2\ s^{-1}$)
h	interelectrode gap (cm)
M_1	first moment of the response, defined by Equation 3
M_2	second moment of the response, defined by Equation 4
$Q = V/h$	volumetric flow rate per unit interelectrode gap ($cm^2\ s^{-1}$)
r	radius (cm)
$(Re) = V/h\nu = Q/\nu$	channel Reynolds number
$(Re)_{\phi_L} = \omega r^2/\nu$	local rotational Reynolds number
$\bar{t}$	plug flow residence time, defined by Equations 6 or 7 (s)
V	volumetric flow rate ($cm^3\ s^{-1}$)
τ	mean residence time of marked fluid (s)
ν	kinematic viscosity ($cm^2\ s^{-1}$)
ω	angular velocity ($rad\ s^{-1}$)

Subscripts

i	inner
I	inflow
o	outer
O	outflow

1. Introduction

The capillary gap (disc-stack) cell [1] and pump cell [2] normally operate with radial outflow of electrolyte between closely-spaced parallel disc electrodes, the principal difference being that, in the pump cell, every alternate disc is rotated. It has been shown [3, 4] that the specificities of some electro-organic syntheses in these two kinds of cell may be markedly different under the same nominal conditions, and it has been hypothesized [3] that the difference is due to the different mixing conditions prevailing close to the electrode. Certainly the tangential shear in the pump cell produces a different distribution of mass transfer coefficient [13, 14, 19] to that in a geometrically identical capillary gap cell [13, 20].

Since the mixing environment in a cell can be characterized in terms of the space–time history of injected marker species [4], an electrochemical analogue [5] of the conventional dye-injection technique of chemical engineering [6] can be used to investigate the local environment in electrochemical reactors [7, 8]. A necessary prerequisite is the simplest mathematical model which will adequately represent the local conditions in the cell. Experience has shown [4, 5, 7, 8, 10, 21] that highly sophisticated models do not lead to unambiguous results, since there is not enough statistical redundancy in the experimental data to differen-

0021–891X/79/040437–08 $02·80/0

tiate between alternative multi-parameter descriptions. A simple model for radial flow between parallel discs was developed in Part I of this paper [9]; briefly, it assumes dispersive plug flow in the radial direction of a slab of fluid of undetermined thickness close to each electrode. While work is progressing on higher level models [12], in the present description no mass exchange is allowed between this wall layer and the bulk of the fluid. The effects of the real velocity profile, the deceleration of the flow, of stochastic fluctuations and other disturbing influences are lumped together in a term which represents dispersion in the radial direction, i.e. the direction of mean mass flow. If a pulse of concentration, e.g. of Cu^{2+} ions, is created at the disc surface, then this will be convected downstream and will disperse as it goes, such that a concentration detector buried in the wall further downstream will show a response distributed in time.

The mean residence time, τ, and dispersion, $\bar{D}$, of the electrogenerated species can be estimated from the response using the expressions [9] (Part I)

$$\tau = M_1 \tag{1}$$

and

$$\bar{D}_O = \frac{(r^2 - r_i^2)}{4M_1\{1 + [(r^2 + r_i^2)/(r^2 - r_i^2)]\,[M_1^2/(M_2 - M_1^2)]\}} \tag{2}$$

where M_1 and M_2 are the normalized moments of the response, defined by

$$M_1 = \int_0^\infty tc\,dt \Big/ \int_0^\infty c\,dt \tag{3}$$

and

$$M_2 = \int_0^\infty t^2 c\,dt \Big/ \int_0^\infty c\,dt. \tag{4}$$

Here $c(t)$ is the concentration of the injected marker species, and r_i and r are the radii of the injector and detector electrodes in the wall.

In Part I it was shown that

$$M_1 = -\frac{(r^2 - r_i^2)}{4(1 - Q/4\pi\bar{D})\bar{D}} \tag{5}$$

so that if $Q \gg 4\pi\bar{D}$

$$M_1 = \tau_O \simeq \pi(r^2 - r_i^2)/Q = \bar{t} \tag{6}$$

which is the volumetric residence time. However experiment shows that M_1 can be one or two orders of magnitude larger that $\bar{t}$, which first led to the concept of a creeping wall layer highly segregated from the bulk flow.

For the case of radial *inflow* the analagous expressions are:

$$\bar{D}_I = \frac{(r_o^2 - r^2)}{4M_1\{[(r_o^2 + r^2)/(r_o^2 - r^2)]\,[M_1^2/(M_2 - M_1^2)] - 1\}} \tag{7}$$

and

$$\bar{t} = \pi(r_o^2 - r^2)/Q \tag{8}$$

where r_o is the radius of the injector at the periphery of the disc.

As mentioned above, mass exchange between the creeping wall layer and the core is not allowed in the present model, which is a deficiency, however the mathematical difficulties are considerable when this feature is introduced and related studies [7, 8, 10, 21] have suggested that the additional degree of understanding obtained from a more sophisticated model is not always great.

2. Experimental

Fig. 1 shows a schematic diagram of the model cell used in this work. Each disc was cast in epoxy resin with four concentric rings of nickel foil at diameters of 60, 78, 96 and 114 mm and two rings of copper at diameters of 40 and 136 mm. The discs were faced-off on a lathe. The lower disc had a central entry/exit port 18 mm in diameter and was rigidly fixed to an ordinary chemical tripod glued to the base of a square glass tank which was filled with an indifferent electrolyte. The upper disc, also beneath the liquid surface, was suspended from a shaft which could be rotated; vertical adjustment of the shaft allowed the gap to be altered between 0·6 and 4·3 mm. Taken in pairs, the metal rings formed complementary anodes and cathodes of marker or detector circuits; leads from the electrodes of the rotating disc were connected to small annular mercury pool contacts set along the shaft so that electrical connections could be made. A tube was fixed to the central bore of the lower disc so that a small circulating pump could withdraw electrolyte from the tank and pump it radially outwards through the model cell; radial inflow was achieved by reversing the pump.

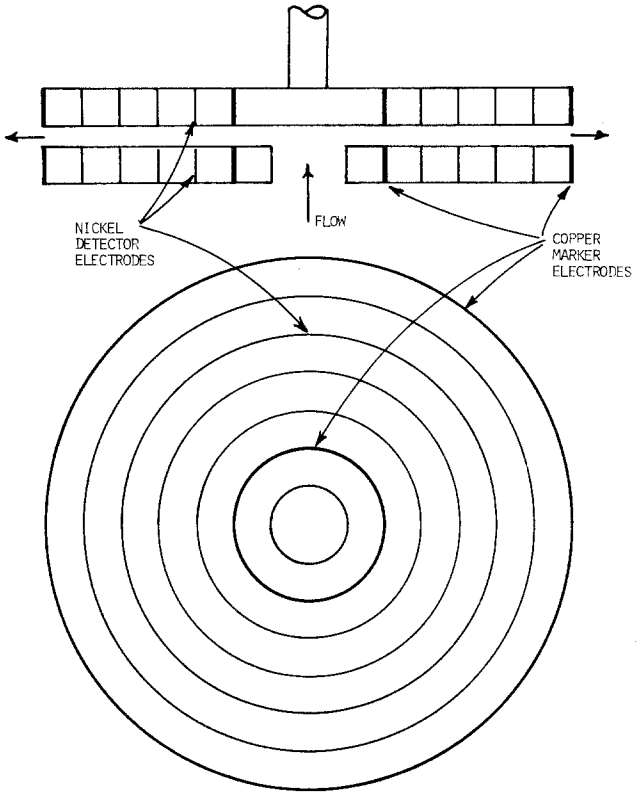

Fig. 1. Schematic diagram of model cell.

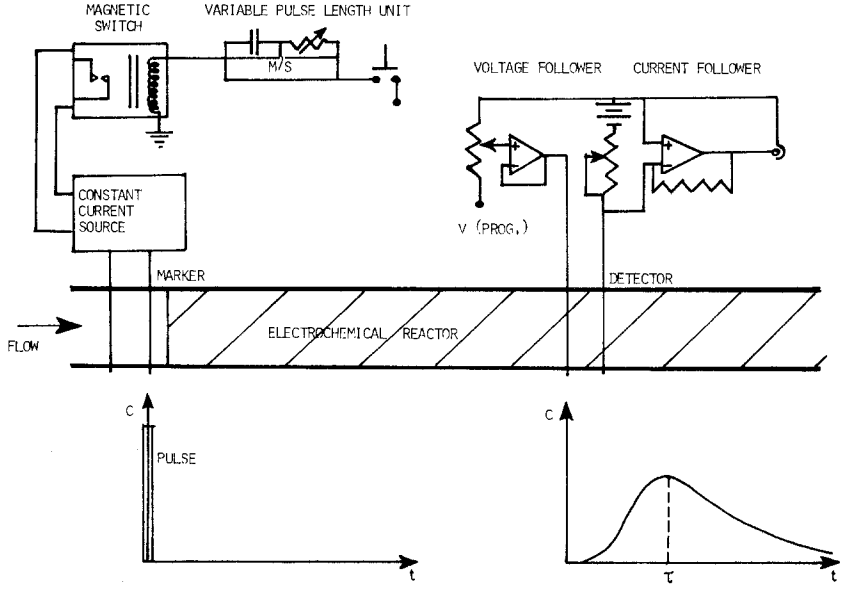

Fig. 2. Schematic diagram of marker pulse apparatus.

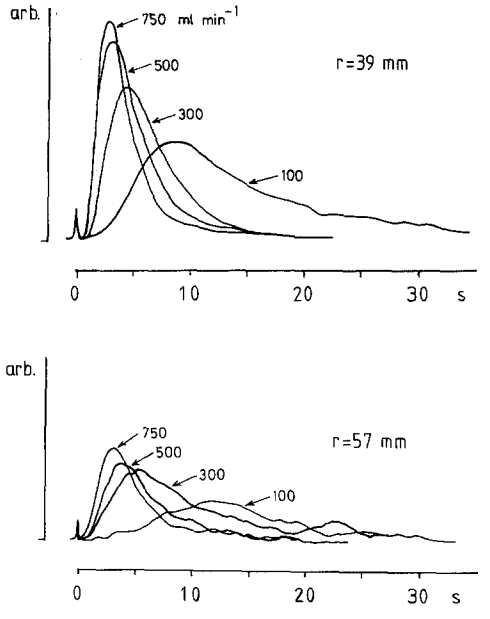

Fig. 3. Response curves for radial outflow in capillary gap configuration, gap 0·6 mm, detectors at radii of 39 and 57 mm.

The marker-pulse technique has been described elsewhere [5, 7, 8]. Briefly, (Fig. 2) a voltage pulse (of about 10 ms duration) was applied between opposed copper rings, which injected copper ions into solution on the anode side. These convected in the direction of the flow. Each of the pairs of nickel electrodes was maintained at the potential of the diffusion limiting current by means of a current follower/voltage follower circuit, the output potential then being an analogue of concentration. The voltage–time curves were recorded on a Bryans 26000 y–t recorder, a Racal Store 4 tape recorder, or were acquired directly by the PDP 11/55 computer of the Data Analysis Centre. Recorded data were digitized off-line at a later date. but all numerical processing to obtain the moments was performed in the computer.

The responses to pulses were obtained for different conditions of gap, volumetric flow rate, rotation rate and direction of flow, the normalized moments and estimates of $\bar{D}$ (using Equation 2 or 7, as appropriate) being returned to the VDU in the laboratory. The regression of derived data was performed by hand calculator, the PDP 11/55 or the University's ICL 1907, depending on the degree of difficulty.

As can be seen from Fig. 3, the quality of the transients degraded with increasing radius and decreasing flow rate since the current due to marker ions is extremely small. Signal averaging [10] and correlation [11] techniques can be used to improve the signal-to-noise ratio, but in these experiments the channel and rotational Reynolds numbers could not be increased beyond $1{\cdot}6 \times 10^5$ and $1{\cdot}7 \times 10^5$ respectively without loss of signal.

3. Results

By definition [6] the first moment of the response to a delta-function input is the mean residence time, τ, of the marked material (Equations 1 and 3). It was immediately apparent from the first responses obtained that τ was much longer than the volumetric residence time, $\bar{t}$, calculated from Equations 6 or 8 using the volumetric flow rate through the cell. In fact in the capillary gap configuration (no rotation) the ratio $(\tau/\bar{t})$ was sometimes as large as 100, depending on flow rate. For this reason it is impossible to use the volumetric flow rate in equations such as Equation 33 in Part I, to estimate $\bar{D}$, and the simplest useful model is one of a slow dispersive plug flow of undetermined thickness creeping down the wall in contact with a faster 'core' plug flow. $\bar{D}$ can then be estimated from Equations 2 or 7, the mean flow rate for the marked material being implicit in M_1.

As shown in Fig. 4, despite the noise in the transients (particularly at large radii and low flow rates, Fig. 3) it is possible to correlate $(\tau/\bar{t})$ versus channel Reynolds number, $(Re) = V/h\nu = Q/\nu$, for different interelectrode gaps and detectors at different radii in the capillary gap configuration (no rotation). Likewise, in the pump cell case, correlations can be obtained with (Re) and the local rotational Reynolds number, $(Re)_{\phi_L} = \omega r^2/\nu$ (Table 1). In general the responses for the pump cell (rotational) cases were much sharper and easier to identify than those for the non-rotational cases (Fig. 4, Part I [9]); this made determination of the moments easier, although the criterion for truncation of the tail remained a problem. Agreement between experiments at different gap setting, volumetric flow rates, rotational speeds and for detection at different radii was surprisingly good, considering the approximate nature of the model and the noisiness of the signal, the correlation coefficient in all but a few cases being greater than

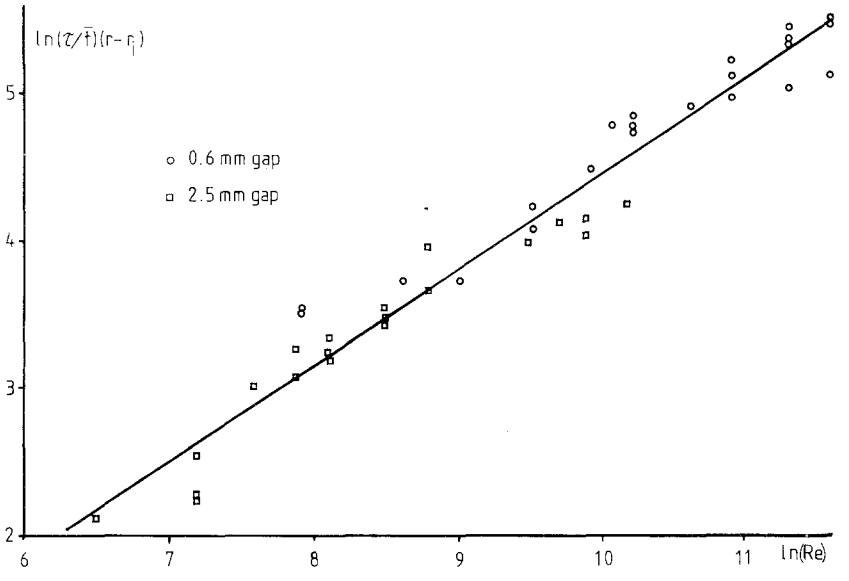

Fig. 4. Regression of space–time data for radial outflow in capillary gap configuration.

0·93. Fig. 5, for example, shows the regression lines for experiments at four different gap settings, four different radii, rotational speeds from 100–500 rev min^{-1} and volumetric flow rates from 0·1–4·5 l min^{-1}. The individual data points are so overlapped that they are not shown.

The regression equations obtained from experimental data are tabulated in Table 1.

4. Discussion

4.1. *General*

Many empirical correlations were attempted, but only those shown in the figures and Table 1 were at all successful. The fact that they all imply a length dependence shows that the model is not

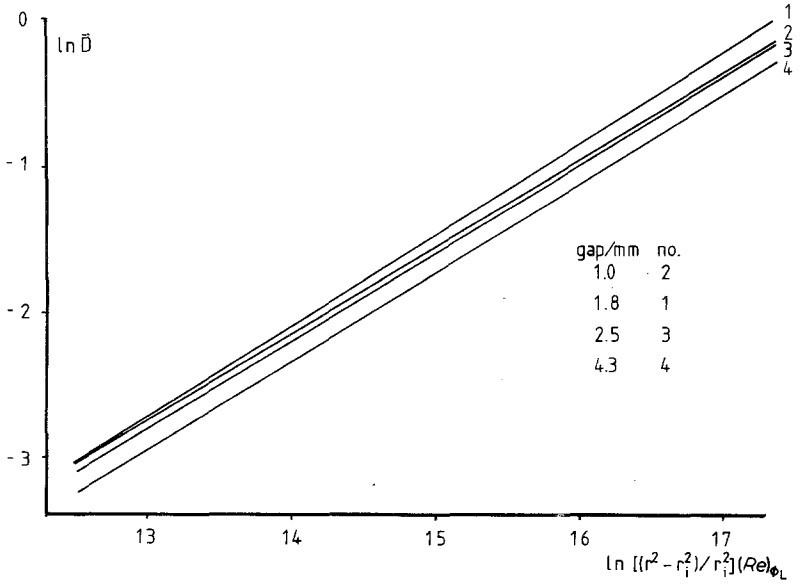

Fig. 5. Regression of dispersion data for radial outflow in pump cell configuration.

Table 1. Regression equations for experimental data

Cell	*Flow direction*	*Equation*	*Correlation coefficient*	*Number*
capillary gap	out	$(\tau/\bar{t}) = 5{\cdot}95 \times 10^{-2} \dfrac{r_i}{(r - r_i)} (Re)^{0{\cdot}66}$	0·98	9
	in	$(\tau/\bar{t}) = 2{\cdot}80 \times 10^{-1} \dfrac{r_o}{(r_o - r)} (Re)^{0{\cdot}348}$	0·84	10
	out	$\bar{D} = 2{\cdot}752 \times 10^{-4} \dfrac{(r^2 - r_i^2)}{r_i^2} (Re)^{0{\cdot}438}$	0·93	11
	in	$\bar{D} = 0{\cdot}236 \times 10^{-5} \dfrac{(r_o^2 - r^2)}{r_o^2} (Re)^{1{\cdot}222}$	0·93	12
pump cell (rotor)	out	$(\tau/\bar{t}) = 2{\cdot}805 \times 10^{4} \left[\dfrac{(r^2 - r_i^2)}{r_i^2} (Re)_{\phi_L}\right]^{-0{\cdot}596}$	0·98	13
	in	$(\tau/\bar{t}) = 1{\cdot}356 \times 10^{3} (Re)^{0{\cdot}376} (Re)_{\phi_L}^{-0{\cdot}749}$	0·96	14
	out	$\bar{D} = 1{\cdot}766 \times 10^{-4} \left[\dfrac{(r^2 - r_i^2)}{r_i^2} (Re)_{\phi_L}\right]^{0{\cdot}606}$	0·97	15
	in	$\bar{D} = 2{\cdot}777 \times 10^{-2} (Re)^{1{\cdot}402} (Re)_{\phi_L}^{1{\cdot}251}$	0·91	16
pump cell (stator)	out	$(\tau/\bar{t}) = 5{\cdot}622 \times 10^{2} \left[\dfrac{(r^2 - r_i^2)}{r_i^2} (Re)\right]^{-0{\cdot}369}$	0·82	17
	in	$(\tau/\bar{t}) = 1{\cdot}105 (Re)^{0{\cdot}808} (Re)_{\phi_L}^{-0{\cdot}457}$	0·97	18
	out	$\bar{D} = 3{\cdot}177 \times 10^{-10} (Re)^{1{\cdot}472} (Re)_{\phi_L}^{0{\cdot}396}$	0·95	19
	in	$\bar{D} = 3{\cdot}838 \times 10^{-6} (Re)^{0{\cdot}531} (Re)_{\phi_L}^{0{\cdot}589}$	0·95	20

strictly applicable, but this was always recognised, since clearly there must be mass exchange with the faster fluid. Nevertheless the different correlations do allow the collapse of data from experiments under widely different conditions (e.g. a ratio of 7·1 : 1 in gap, 5 : 1 in rotation speed, 45 : 1 in volumetric flow rate and 2·85 : 1 in radius) showing that they do have some physical significance. Further, by definition, $M_1 = \tau$, i.e. M_1 is a direct measure of the residence time of *electrogenerated* species in the vicinity of the wall, which is a paramount parameter in determining the course of electrosynthetic reactions [4].

As discussed in Part I, even in this simplest model the degree of mathematical difficulty is such that the only analytical technique available is moment analysis. The zeroth and first moments can be estimated with fair accuracy, but truncation becomes a problem for the second and higher moments since the moment becomes dominated by contributions from the 'tail'. Nevertheless, the fact that correlations could be obtained over a range of radii suggests that, despite the sometimes poor signal quality (Fig. 3) the reduced data is good enough for present purposes.

4.2. *Capillary gap cell*

As shown in Table 1 and Fig. 4 the ratio $(\tau/\bar{t})$ is inversely proportional to distance between the marker electrode and the detector. This implies mixing between the marked and unmarked (fast and slow) streams, which cannot be accommodated explicitly with the present model. Also as (Re) increases so does $(\tau/\bar{t})$, showing that the degree of segregation between the two streams increases, although, of course, as (Re) increases τ decreases, as shown qualitatively by Fig. 3 or explicitly, for example, by Equation 9 using Equation 6 and the definition of (Re):

$$\tau = 5{\cdot}95 \times 10^{-2} \frac{\pi r_i (r_i + r) (Re)^{-0{\cdot}34}}{\nu}.$$

Paradoxically, pumping harder decreases the resi-

Table 2. Comparison of parameters for radial inflow and radial outflow, capillary gap configurations

Reynolds number $(Re) = V/h\nu$	$r_o/r_i = 5$		$r_o/r_i = 10$	
	(τ_O/τ_I)	$(\bar{D}_O/D_I)$	(τ_O/τ_I)	$(\bar{D}_O/\bar{D}_I)$
10^3	0·37	12·96	0·18	51·85
3×10^3	0·52	5·48	0·26	21·91
10^4	0·75	2·13	0·38	8·53
3×10^4	1·06	0·91	0·53	3·60
10^5	1·53	0·35	0·77	1·40
2×10^5	1·92	0·20	0·96	0·81

dence time of the electrogenerated species close to the electrodes, but also increases the segregation of these species from the 'core' fluid, with obvious chemical consequences. The dispersion of electrogenerated species increases with length and Reynolds number, as would be expected for a mixing process.

In the case of radial inflow similar comments apply although, judging from the lower exponent for (Re), the degree of segregation of fast and slow streams would appear to be less. However, the ratios, (τ_O/τ_I), and $(\bar{D}_O/\bar{D}_I)$, are functions of geometry as well as Reynolds number, as Table 2 emphasizes, thus the requirements of a reaction (long or short residence time, high or low mixing) in principle can be accommodated to a degree by choice of radius ratio, flow rate, gap and flow direction.

4.3. *Pump cell*

First of all it must be recognised that there are two different hydromechanical environments; that at the rotor and that at the stator. Fig. 6, following Haynes [15], is a sketch of the axial and tangential velocity profiles in air for radial outflow between differentially rotating planes; at the rotor the tangential velocity gradient is very high, while at the stator it is small unless the gap is very small, when Couette flow is approximated. This picture has been confirmed for the pump cell by mass transfer studies [13, 14]; since the Schmidt number is so high for aqueous systems the rotor behaves essentially as a free disc in a semi-infinite fluid down to gaps of the order of 0·1 mm. One would therefore expect $\bar{D}$ and $(\tau/\bar{t})$ to be functions of $(Re)_{\phi_L}$ rather than (Re), as confirmed for outflow by Table 1. In the case of inflow, however, a strong interaction with the impressed flow seems likely, and Table 1 suggests that this is so; attempts are being made to model the fluid field explicitly [18].

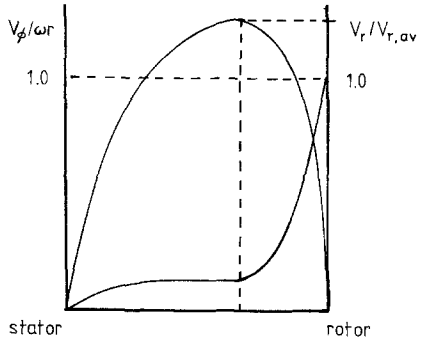

Fig. 6. Schematic diagram of tangential and 'radial' (truly axial) velocity profiles, V_ϕ and V_r, in the pump cell case. (After Haynes [15]).

Due to the smaller tangential velocity gradient at the stator, a smaller dependence on $(Re)_{\phi_L}$ would be expected. Indeed, it is (Re) which is the more important in this case, although a strong degree of interaction is implied by Table 1. Detailed comments will be reserved until the effect of flow direction on the velocity field has been investigated.

4.4. *Effect on organosyntheses*

The difference in environment close to an electrode is important in mixing-sensitive reactions. Such a reaction is the methoxylation of furan carried out indirectly via the electrolysis of ammonium bromide [16]. Here the 2,5-dibromo intermediate is rapidly methoxylated close to the bromine-generating anode with the production of HBr. If the mixing near the anode is not good the

locally low pH can lead to destruction of the product which is the cyclic acetal 2,5-dihydro-2,5-dimethoxyfuran. Systematic studies [3] carried out in a number of types of cell showed that a bipolar pump cell operating normally (with radial outflow) gave the highest specificity of product, about 95%, even at concentrations of product greater than 1 mol dm^{-3}. This can only be because the good mixing in the cell prevented the anolyte layer becoming very acid. Other reactions which have been examined in this way [3] are the electro-hydrodimerization of acrylonitrile, the dimerization of diethyl malonate and the indirect oxidation of benzyl alcohol. The distribution of products can be explained similarly, in terms of the local mixing in the cells.

5. Conclusions

This work has shown that the mixing environment close to an electrode can be characterized by physical means. The simplest model which can be used is that of a slow, creeping flow along the electrode face, highly segregated from the core flow. At the present level of modelling mass exchange between the creeping flow and the core can not be accommodated, therefore the expressions in Table 1 can only be taken as approximate. Nevertheless they do permit estimates of local conditions to be made, which allows a choice of operating conditions suitable for the sequence of desired chemical and electrochemical reactions. It has been shown [3, 4] that tailoring the physical conditions to the needs of a chemical reaction is perfectly possible.

Work is progressing on improved models [12], however, it should be recognised that fitting a multi-parameter description to experimental data may produce answers which look convincing but have no real significance, particularly in view of the mathematical complexity of the derived equations. It may yet prove that the limited model developed in these papers is still the most suitable for general use in the semi-quantitative characterization of reactors with radial flow.

References

[1] F. Beck and H. Guthke, *Chim. Ingnr. Techn.* 4 (1969) 943.
[2] M. Fleischmann, R. E. W. Jansson, G. A. Ashworth and P. J. Ayre, British Prov. patent appl. 18 305 (1974).
[3] N. Tomov, PhD thesis, 'Southampon University (1978).
[4] M. Fleischmann and R. E. W. Jansson, Keynote Lecture, *AIChE Meeting*, Atlanta, Georgia (1978).
[5] I. H. Justinijanović, PhD thesis, Southampton University (1975).
[6] O. Levenspiel, 'Chemical Reaction Engineering', Wiley, New York (1962).
[7] Z. Ibrisagic, PhD thesis, Southampton University (1977).
[8] J. Ghoroghchian, PhD thesis, Southampton University (1978).
[9] M. Fleischmann and R. E. W. Jansson, *J. Appl. Electrochem.* 9 (1979) 427.
[10] R. J. Marshall and R. E. W. Jansson, *J. Chem. Technol. Biotechnol.*, to be published.
[11] J. Overstall and R. E. W. Jansson, submitted to *J. Appl. Electrochem.*
[12] M. Fleischmann and R. E. W. Jansson, unpublished work.
[13] G. A. Ashworth, PhD thesis, Southampton University (1977).
[14] R. E. W. Jansson and G. A. Ashworth, *Electrochim. Acta.* 22 (1977) 1301.
[15] C. M. Haynes, PhD thesis, Sussex University (1973).
[16] R. E. W. Jansson and N. R. Tomov, *Chemy. Ind. No. 3* 96 (1978).
[17] J. Ghoroghchian, R. E. W. Jansson and R. J. Marshall, submitted to *Electrochim. Acta.*
[18] R. E. W. Jansson, unpublished work.
[19] R. E. W. Jansson and R. J. Marshall, *Chem. Engnr.* 315 (1976) 769.
[20] G. A. Ashworth and R. E. W. Jansson, *Electrochim. Acta* 22 (1977) 1295.
[21] F. Sarfarazi, PhD thesis, Southampton University (1979).